

like to suggest looking at  $(\bar{K}+N)$  as a breakup of  $\Sigma$  in (14), but in view of the  $Y_1^*$  and  $Y_1^{**}$  contributions this would be particularly difficult. We also note that the experiments on boson systems (10), (11), and (12) necessarily involve looking at breakup systems which are fast in the lab and, thus, more difficult to measure. In view of these difficulties, it may be guessed that most of these experiments will require highly refined equipment triggered on the processes in question. But it is just possible that some could be performed as a byproduct of large bubble-chamber experiments (note 4% estimate in  $p \rightarrow N + \pi$  case above). As another example, reaction (14) could be examined at say 5 BeV: Consider only events associated with one very fast  $\pi$  in the lab. If several hundred slow charged  $\Sigma$ 's were found, determining  $d\sigma^{\text{II}}(\Delta)$ , one could plot individual

$(\Lambda + \pi)$  events, in a suitable  $\omega$  interval, as a function of  $\Delta$  weighted by  $1/d\sigma^{\text{II}}(\Delta)$ . There might be several tens of such events. The distribution should be constant. The weighted  $\Lambda + \pi$  events for all suitable  $\Delta$  should also be plotted against  $\omega$  to test the  $k^3$  dependence. The charged  $Y_1^*$  distribution should also be examined to show, with luck, that the low  $\omega$   $(\Lambda + \pi)$  events of interest were not the tail of that distribution. Passing all these tests,  $d\sigma^{\text{III}}/d\sigma^{\text{II}}$  would be interpretable by means of (4) in terms of  $g_{\Lambda\Sigma\pi}^2$ .

ACKNOWLEDGMENTS

The author would like to thank Dr. B. Desai and Professor A. N. Mitra for useful suggestions and Y. Li and J. Higgins for assistance.

$Y_0^*$  and the Low-Energy  $\bar{K}N$  Interaction

Y. FUJII

Department of Physics, College of Science and Engineering, Nihon University, Surugadai, Tokyo, Japan

(Received 26 March 1963; revised manuscript received 6 May 1963)

An analysis is attempted on the low-energy  $\bar{K}N$  data by assuming that the  $Y_0^*$  is an  $S$ -wave  $\bar{K}N$  bound state. Two tentative sets for the scattering lengths are obtained which are similar to that of Akiba and Capps, and fit all the low-energy data reasonably well.

THE two solutions obtained by Humphrey and Ross<sup>1</sup> for the  $\bar{K}N$  scattering lengths suggest the existence of a Dalitz-Tuan type resonance<sup>2</sup> in the  $I=0$  state. It is, however, not yet conclusive quantitatively whether it corresponds to the  $Y_0^*$  recently observed.<sup>3,4</sup> There is some indication that the imaginary part of the isosinglet scattering length is too large for the above identification to be valid, especially in the first solution (hereafter referred to as HR-I).<sup>5-8</sup> Also it seems rather difficult to obtain a unique solution from the data on low-energy  $K^-p$  reactions only.<sup>9</sup> In this note we shall make an analysis on the low-energy  $\bar{K}N$  data assuming that the  $Y_0^*$  has a spin  $\frac{1}{2}$  and even parity with respect to  $\bar{K}N$ .

In the zero-range approximation the (real) phase

shift  $\delta$  of isosinglet  $\pi\Sigma$  scattering below the  $\bar{K}N$  threshold is given by<sup>2,8,10</sup>

$$\frac{q}{\bar{q}} \cot \delta(\kappa) \approx - \frac{1}{z} \frac{\kappa_0 \kappa - \kappa_r}{\kappa_r \kappa - \kappa_0}, \tag{1}$$

where  $q$  is the  $\pi\Sigma$  momentum,  $\bar{q}$  being its value at  $\bar{K}N$  threshold;  $\kappa$  may be taken as the average of the absolute value of the (imaginary)  $K^-p$  and  $\bar{K}^0n$  momenta, and

$$\kappa_r = -(a_0 + b_0 z)^{-1}, \tag{2a}$$

$$\kappa_0 = -(a_0 - b_0/z)^{-1}, \tag{2b}$$

where  $A_0 = a_0 + ib_0$  is the isosinglet  $\bar{K}N$  scattering length,  $z$  being given by

$$z = \tan \varphi,$$

with  $\varphi$ , the value of  $\delta$  at  $\bar{K}N$  threshold. At  $\kappa_r$  and  $\kappa_0$  there occur a peak and a dip, respectively, in the  $\pi\Sigma$  scattering cross section.

The pole at  $\kappa_0$  in the inverse of the  $\pi\Sigma$  scattering amplitude is peculiar to a two-channel problem; an example of such a pole can be easily found in a simple chain approximation model.<sup>10</sup> The location of  $\kappa_0$  varies

<sup>1</sup> W. E. Humphrey and R. R. Ross, Phys. Rev. **127**, 1305 (1962).

<sup>2</sup> R. H. Dalitz and S. F. Tuan, Ann. Phys. (N. Y.) **10**, 307 (1960).

<sup>3</sup> M. H. Alston, L. W. Alvarez, P. Eberhard, M. L. Good, W. Graziano, H. K. Ticho, and S. G. Wojcicki, Phys. Rev. Letters **6**, 698 (1961).

<sup>4</sup> G. Alexander, G. R. Kalbfleisch, D. H. Miller, and G. A. Smith, Phys. Rev. Letters **8**, 447 (1962).

<sup>5</sup> Y. Miyamoto, Progr. Theoret. Phys. (Kyoto) **27**, 203 (1962).

<sup>6</sup> T. Akiba and R. H. Capps, Phys. Rev. Letters **8**, 457 (1962).

<sup>7</sup> T. Akiba, Progr. Theoret. Phys. (Kyoto) **29**, 439 (1962).

<sup>8</sup> Y. Fujii, Progr. Theoret. Phys. (Kyoto) (to be published).

<sup>9</sup> For example, the observable results calculated from Humphrey and Ross's two solutions are distinguished with each other mainly by a delicate energy dependence of the ratio  $\Sigma^-/\Sigma^+$ .

<sup>10</sup> Y. Fujii and M. Uehara, Suppl. Progr. Theoret. Phys. (Kyoto) **21**, 138 (1962).

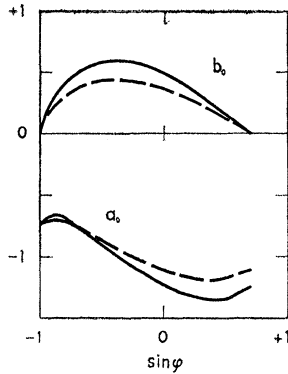


FIG. 1. Plots of  $a_0$  and  $b_0$  versus  $\sin \varphi = z/(1+z^2)^{1/2}$ . The solid and broken curves correspond to  $W_r = 1415$  and  $1410$  MeV, respectively. Units are used in which the pion mass is unity.

depending upon  $z$ , and accordingly the cross section exhibits some typical patterns:

(a) For  $z > 0$ , we have  $0 < \kappa_0 < \kappa_r$ , to give a cross section with a dip between the peak and  $\bar{K}N$  threshold, at which there occurs an upward cusp.

(b) For  $b_0/a_0 < z < 0$  with  $a_0 < 0$ , and for  $z < 0$  with  $a_0 > 0$ ,  $\kappa_0$  is negative to give no observed dip. The cross section falls off steeply at  $\bar{K}N$  threshold (a decreasing round step).

(c) For  $z < b_0/a_0$  with  $a_0 < 0$ , we have  $\kappa_r < \kappa_0$ , to give a cross section with a dip at the lower energy side of the peak. The behavior at  $\bar{K}N$  threshold is the same as in (b). There might be the case where  $\kappa_0$  is larger than the value corresponding to  $\pi\Sigma$  threshold to give no observed dip.

Considering that these detailed behaviors of the cross section are ignored in the present experiments, we introduce, as a measure of the width, an energy  $W_1$  (smaller than  $W_r$ , the resonance energy), at which the cross section amounts to about half-maximum, to give

$$\frac{1}{z} \frac{\kappa_0 \kappa_1 - \kappa_r}{\kappa_r \kappa_1 - \kappa_0} = 1, \quad (3)$$

where  $\kappa_1$  is the corresponding "momentum."

If  $\kappa_r$  and  $\kappa_1$  are given, Eqs. (2) and (3) can be solved for  $a_0$  and  $b_0$ , which have been plotted versus  $\sin \varphi$ ,<sup>11</sup> for  $W_r = 1410$  and  $1415$  MeV, with  $W_1 = 1380$  MeV in both cases. A smaller  $W_r$  or a larger  $W_1$  gives a smaller  $b_0$ . We find that  $b_0$  is "small": It is far smaller than 1.94 in HR-I<sup>12</sup>; even the maximum is somewhat smaller than 0.68 in HR-II.  $a_0$  is negative and is larger in magnitude than the values in HR.

Now we are going to investigate what the obtained  $A_0$  implies about the low-energy  $\bar{K}N$  data. First, we shall try to determine  $A_1$  using some available data.

An equation for  $A_1$  is obtained from the expression for a branching ratio of hyperons produced from  $K^-p$  at rest<sup>2</sup>:

$$\frac{|1 + \kappa_t A_1|^2}{b_1} = \frac{|1 + \kappa_t A_0|^2}{b_0} \mu \equiv 2X, \quad (4)$$

<sup>11</sup> More precisely,  $\sin \varphi = z/(1+z^2)^{1/2}$ .

<sup>12</sup> Units are used in which the pion mass is unity.

with

$$\mu = \frac{3\Sigma^0}{\Sigma^- + \Sigma^+ - 2\Sigma^0 + \Lambda} \Big|_{\text{at rest}},$$

where  $\kappa_t$  is the absolute value of the imaginary  $\bar{K}^0 n$  momentum corresponding to  $K^-p$  threshold. Among the in-flight data, we choose  $\sigma(\Sigma^-\pi^+) + \sigma(\Sigma^+\pi^-)$  as most reliable. At an energy which is high enough so that the  $\bar{K}^0 n - K^-p$  mass difference is neglected and is low enough so that the effective-range terms are unimportant, we have

$$|1 - ikA_1|^2/b_1 = 4\pi/k\sigma_1(k) \equiv 2(Y+k), \quad (5)$$

where  $k$  may be taken as the average of the momenta in the  $K^-p$  and  $\bar{K}^0 n$  systems,  $\sigma_1(k)$  being the isotriplet total production cross section. The latter can be evaluated as

$$\sigma_1 = -\sigma_{1\Sigma} = \frac{1}{\nu} \left[ 2(\sigma_{\Sigma^-} + \sigma_{\Sigma^+}) - \frac{24\pi}{3k} \frac{b_0}{|1 - ikA_0|^2} \right],$$

where  $\nu$ , the ratio of the cross section for the isotriplet  $\Sigma$  production  $\sigma_{1\Sigma}$  to  $\sigma_1$ , is considered as constant in the zero-range approximation. Equations (4) and (5) represent circles in the plane of  $A_1^{-1}$ ; the center and the radius are  $-\kappa_t - iX$  and  $X$  for (4),  $-iY$  and  $(Y^2 - k^2)^{1/2}$  for (5), respectively. The condition for the intersection of these circles with each other is given by

$$4k^2X^2 - 4(k^2 + \kappa_t^2)XY + (k^2 + \kappa_t^2)^2 \leq 0,$$

which represents a portion of the  $XY$  plane surrounded by one of the hyperbolas; only the quadrant  $X > 0$ ,  $Y > 0$  need be considered.

This portion is mapped onto a similar one in the  $\mu\nu$  plane; the bottom of the hyperbola lies at

$$\mu = k^{-1}(k^2 + \kappa_t^2)b_0|1 + \kappa_t A_0|^{-2},$$

$$\nu = (k^2/\pi)\sigma_{1\Sigma}(k).$$

The variables  $\mu$  and  $\nu$  are expressed in terms of the branching ratios relating to the neutral hyperons produced from  $K^-p$  at rest:

$$\begin{pmatrix} \mu \\ \nu \end{pmatrix} = \begin{pmatrix} 3n(1-m) \\ 1-2n(1-m) \end{pmatrix} \frac{1}{1-2n(1-3m/2)},$$

where

$$m = \Lambda/(\Sigma^0 + \Lambda), \quad n = (\Sigma^0 + \Lambda)/(\Sigma^- + \Sigma^+).$$

Numerical calculations have been made for  $W_1 = 1380$  MeV,  $W_r = 1410$  and  $1415$  MeV,  $\sigma_{\Sigma^-} + \sigma_{\Sigma^+} = 27$  mb at an incident  $K^-$  momentum  $237.5$  MeV/ $c$ .<sup>1</sup> Figure 2 contains the plots of the above-mentioned hyperbola in the  $\mu\nu$  plane. The curves extend most largely for  $\sin \varphi = -0.2 \sim -0.4$  for both values of  $W_r$ . Straight lines corresponding to several values of  $m$  and  $n$  are also plotted. The central values of observations<sup>1</sup>  $m = 0.19$ ,  $n = 0.53$  are represented in the figure by a point denoted

TABLE I. Two tentative solutions for the  $\bar{K}N$  scattering lengths and some of the results.

	A	B
$m$	0.18	0.19
$n$	0.47	0.51
$A_0$	$-0.92+0.43i$	$-0.98+0.59i$
$A_1$	$0.33+0.37i$	$0.30+0.40i$
$\phi$ at 400 MeV/c	$-117^\circ$	$-102^\circ$
$K_1^0/(\Lambda+2\Sigma^0)$ at 237.5 MeV/c	0.61	0.54

by HR, which lies outside any of curves, thus permitting no consistent solution for  $A_1$ . For  $W_r=1415$  MeV, however, the deviation is small, and can be reduced by changing the values within the experimental errors of  $m$ ,  $n$ , and also  $\sigma_{\Sigma^-}+\sigma_{\Sigma^+}$ .

We may tentatively choose two points denoted by A and B, which lie just on the curves for  $\sin\phi = -0.4$  with  $W_r=1410$  and 1415 MeV, respectively, and as close to the point HR as possible. Thus, we obtain the sets of the scattering lengths as listed in Table I. All the data on  $K^-p$  reactions for incident momenta 100~300 MeV/c<sup>4</sup> can be fitted reasonably well, though no systematic attempt has been made to minimize the deviations from experiment. Only the elastic scattering cross section at relatively lower momenta (<200 MeV/c) are smaller than the observed values beyond experimental errors of Ref. 1.<sup>13</sup>

Three remarkable features, which are independent of the possible uncertainties involved in the data used, should be noted: (i) If the ratio  $\Sigma^-/\Sigma^+$  from  $K^-p$  is made to reproduce the observed values, then the phase difference  $\phi$  of the  $\pi\Sigma$  production amplitudes between the  $I=0$  and  $I=1$  states is *negatively* large, as contrasted to HR-I, in accordance with the observed variation of the angular distribution and polarization of  $\Sigma^\pm$  produced from  $K^-p$  around 400 MeV/c<sup>14</sup>; (ii) the branching ratio  $K_1^0/(\Lambda+2\Sigma^0)$  from  $K_2^0p$  is in agreement with observed value 0.4~0.9 at ~240 MeV/c,<sup>15</sup> as contrasted to HR-II; this is due to the fact that the obtained  $a_1$  is smaller than 0.85 in HR-II; (iii) the elastic scattering amplitude interferes destructively with the Coulomb scattering amplitude, as contrasted to HR-II.

The importance of the features (i) and (ii) have been already pointed out by Akiba and Capps.<sup>6</sup> They

<sup>13</sup> For example,  $2\pi \int_{-1}^{0.966} (d\sigma_{e1}/d\Omega) d\cos\theta$  at 137.5 MeV/c amounts only to 52 mb for A, 63 mb for B, compared to the data 75-105 mb (Ref. 1).

<sup>14</sup> M. Ferro-Luzzi, R. D. Tripp, and M. B. Watson, Phys. Rev. Letters 8, 28 (1962); R. D. Tripp, M. B. Watson, and M. Ferro-Luzzi, *ibid.* 8, 175 (1962).

<sup>15</sup> D. Luers, I. S. Mitra, W. J. Willis, and S. S. Yamamoto, Phys. Rev. Letters 7, 255 (1961).

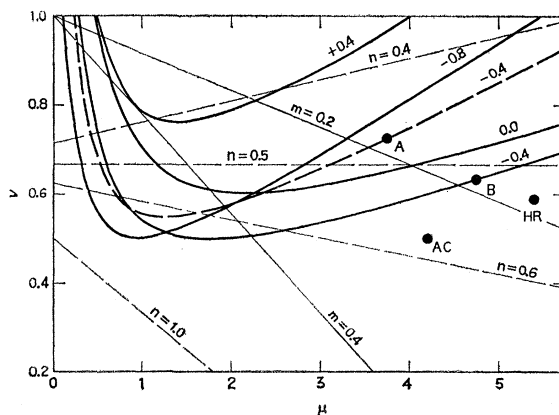


FIG. 2. The point  $(\mu, \nu)$  must lie inside some of curves in order that  $A_1$  is determined consistently. The solid and broken curves correspond to  $W_r=1415$  and 1410 MeV, respectively, with the indicated values of  $\sin\phi$ . Straight lines corresponding to several values of  $m$  and  $n$  are also plotted. The points denoted by HR, AC, A, and B correspond to the observed values in Ref. 1, those used in Ref. 6, and two tentative sets in Table I, respectively.

obtained  $A_0 = -0.92+0.64i$ ,  $A_1 = 0.28+0.43i$ , values which are quite close to those in Table I. The feature (iii), therefore, applies also in their result. It should be emphasized that the present analysis, assuming the  $Y_0^*$  to have spin  $\frac{1}{2}$  and even parity with respect to  $\bar{K}N$ , has led to these results rather automatically.

Akiba and Capps were forced to introduce a small real effective range in the  $I=0$  state. But we have obtained zero-range solutions by choosing appropriate values for  $m$  and  $n$ , possibly within the experimental error. It is noted that their choice<sup>16</sup>  $\nu=0.5$  corresponds to the point in Fig. 2 denoted by AC, which lies below the curves. It seems that the accuracy of the present data gives no determination of the effective range from experiment only.

On the other hand, an analysis in terms of the effective range calculated from some theoretical model will be useful.<sup>7,8</sup> In a preliminary estimate,<sup>8</sup> the (complex) effective range in the  $I=0$  state is rather small in the case of  $S$ -wave  $\pi\Sigma$  channel [odd  $\bar{K}N\Sigma$  parity]. Still it may be important in such a "critical" situation as stated here.

We have chosen  $\sin\phi \sim -0.4$ , as most favorable for the present data. It is, of course, desirable to acquire some knowledge about  $\sin\phi$  from experiments. In this connection it is strongly suggested that a search be made for a possible dip to distinguish among the patterns (a)-(c) described above.

The author wishes to express his sincere thanks to Professor O. Hara, Dr. J. I. Fujita, and Dr. S. Ishida for valuable discussions.

<sup>16</sup>  $\epsilon$  in their paper is related to  $\nu$  by  $\nu = 1 - \epsilon$ .